Optimal design of compact organic Rankine cycle units for domestic solar applications

Barbazza, Luca; Pierobon, Leonardo; Mirandola, Alberto; Haglind, Fredrik

Published in:
Thermal Science

Link to article, DOI:
10.2298/TSCI1403811B

Publication date:
2014

Document Version
Publisher's PDF, also known as Version of record

OPTIMAL DESIGN OF COMPACT ORGANIC RANKINE CYCLE UNITS FOR DOMESTIC SOLAR APPLICATIONS

by

Luca BARBAZZA [a*], ***Leonardo PIEROBON*** [b], ***Alberto MIRANDOLA*** [a], ***and Fredrik HAGLIND*** [b]

[a] Department of Industrial Engineering, University of Padova, Padova, Italy
[b] Department of Mechanical Engineering, Technical University of Denmark, Kongens, Lyngby, Denmark

Original scientific paper
DOI: 10.2289/TSCI1403811B

Organic Rankine cycle turbogenerators are a promising technology to transform the solar radiation harvested by solar collectors into electric power. The present work aims at sizing a small-scale organic Rankine cycle unit by tailoring its design for domestic solar applications. Stringent design criteria, i. e., compactness, high performance and safe operation, are targeted by adopting a multi-objective optimization approach modeled with the genetic algorithm. Design-point thermodynamic variables, e. g., evaporating pressure, the working fluid, minimum allowable temperature differences, and the equipment geometry, are the decision variables. Flat plate heat exchangers with herringbone corrugations are selected as heat transfer equipment for the preheater, the evaporator and the condenser. The results unveil the hyperbolic trend binding the net power output to the heat exchanger compactness. Findings also suggest that the evaporator and condenser minimum allowable temperature differences have the largest impact on the system volume and on the cycle performances. Among the fluids considered, the results indicate that R1234yf and R1234ze are the best working fluid candidates. Using flat plate solar collectors (hot water temperature equal to 75 °C), R1234yf is the optimal solution. The heat exchanger volume ranges between 6.0 and 23.0 dm^3, whereas the thermal efficiency is around 4.5%. R1234ze is the best working fluid employing parabolic solar collectors (hot water temperature equal to 120 °C). In such case the thermal efficiency is around 6.9%, and the heat exchanger volume varies from 6.0 to 18.0 dm^3.

Key words: *solar power*, *renewable energy*, *ORC*, *domestic applications*, *optimization*

Introduction

The exploitation of solar energy in domestic applications has received growing attention due to increasing energy consumption, the scarcity of fossil fuels and environmental concerns. In recent years, many researchers have attempted to utilize solar power to cover part of the heat demand or to convert the heat directly into electricity. Organic Rankine cycle (ORC) turbogenerators are a promising technology to transform the solar radiation harvested by solar collectors into electric power. An ORC unit is in principle similar to a conventional

* Corresponding author; e-mail: luca.barbazza88@gmail.com

steam power module, but it employs an organic working fluid instead of water to convert the thermal energy into work. For kW-size and low temperature applications, an ORC turbogenerator presents several advantages compared to steam plants [1]. Major benefits are the simplicity of the cycle and the possibility of tailoring the working fluid to the specific temperature profile of the heat source. Furthermore, this technology eliminates the problem of turbine blade erosion due to the liquid droplet formation by utilizing a "dry" fluid as the working fluid.

A proper working fluid selection strongly determines the performance of an ORC unit, thus its selection constitutes a crucial step in the design of a highly efficient power module. Hence both academia and industry have given much attention to this topic. As an exemplary case, Tchanche *et al*. [2] investigated the thermodynamic characteristics and performances of 20 fluids for a small-scale solar ORC turbogenerator, and R134a was recommended as the optimal working fluid. For the same application, Quoilin *et al*. [3] demonstrated that solkatherm was the most efficient compound even though high expander volumes had to be accepted. Lakew and Bolland [4] investigated the power production capability of simple ORC modules driven by low-temperature (80-200 °C) heat sources with different refrigerants (R123, R245fa, R134a, R290, R227ea and n-pentane). Larsen *et al*. [5] presented a methodology, based on the principles of natural selection, to determine the optimum working fluid, evaporating pressure and process layout of ORC units for scenarios related to marine engine heat recovery. Included in the solution domain are 109 fluids in sub and supercritical processes. Wang *et al*. [6] conducted a multi-objective optimization of an ORC system with an evolutionary algorithm with two conflicting objective functions, namely, the exergy efficiency and the overall capital cost. The temperature of the exhaust gas was 130 °C, and R134a was selected as the working fluid. The results revealed that the optimal turbine inlet pressure was in the range of 1.8-2.4 MPa, whereas the optimal turbine inlet temperature was located around 90 °C. Pierobon *et al*. [7] performed a multi-objective design optimization of an ORC turbogenerator tailored for off-shore facilities. The genetic algorithm was employed to size plant components (*e. g*. shell-and-tube heat exchangers and turbine); thermal efficiency, compactness, and net present value were the objective functions. The results suggested the use of cyclopentane as the working fluid.

The present work aims at designing a small-scale ORC turbogenerator suited for domestic solar applications. Specific design criteria are therefore high performance, compactness and safe operation. A multi-objective optimization approach modeled by the genetic algorithm is adopted to maximize simultaneously the net power output and the compactness of the ORC module. Operating conditions, environmental impact, safety and commercial availability are part of the working fluid selection process. Turbogenerator compactness is assessed by calculating the sum of the volumes occupied by the heat exchangers (preheater, evaporator, and condenser). Flat plate heat exchangers are selected as heat transfer equipment whose geometry is made part of the optimization routine by implementing well-established correlations for heat transfer coefficients and pressure drops. Notwithstanding the above-mentioned work, the approach in this paper is novel in the sense that it considers the net power output and the total volume as objective functions for the design of highly efficient and compact solar-powered ORC turbogenerators. Moreover, flat plate heat exchangers are embedded in the design process, thus bridging the gap between a mere optimization of the thermodynamic process and the manufacturing of the ORC unit.

Methodology

System description and working fluid selection

A solar-driven organic Rankine cycle system consists of a subsystem collecting the solar radiation and an ORC turbogenerator. Two different solar collector technologies are considered: the flat plate solar collector and the parabolic solar collector. Flat plate solar collectors provide hot water at a temperature up to 80 °C, whereas temperatures higher than 120 °C can be attained with parabolic solar collectors.

Figure 1(a) shows the five components constituting the ORC power module: liquid pump, preheater, evaporator, expander and condenser. The pump pressurizes the liquid fluid which is injected into the preheater and further heated in the evaporator to produce vapor that is then expanded in a turbine connected via a shaft to an electric generator. Finally, the vapor discharged at the outlet of the expander is condensed and sucked up by the pump to complete the cycle. Figure 1(b) illustrates the *T-s* diagram with the thermodynamic states of an exemplary solar-driven ORC power module using R1234yf as the working fluid; the temperature profiles of the heat source and of the cooling water are also depicted. Note that the minimum temperature difference of the heating process is located at the inlet of the evaporator.

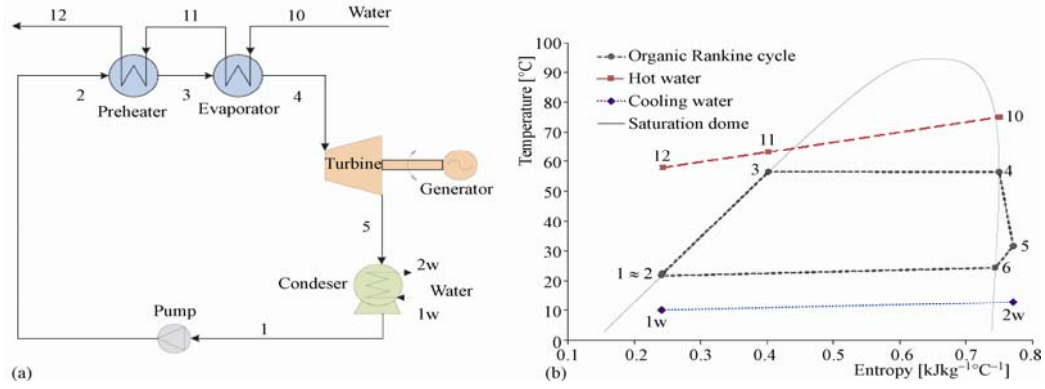

Figure 1. Organic Rankine cycle turbogenerator; (a) System layout. The hot source stream is liquid water coming from the solar collectors; (b) Saturation dome of R1234yf in a *T-s* diagram, showing part-load the thermodynamic cycle state points for one exemplary systems. The red and blue lines represent the temperature profiles of the hot stream and of the cooling water

As regarding the working fluid selection, an optimal candidate should provide high design-point and part-load performances, as well as be economical, nontoxic and inflammable [8]. Furthermore, the growing attention to environmental impact limits the number of fluids under investigation as ideal candidates should exhibit a low ozone depleting potential (ODP) and low global warming potential (GWP). Considering the aforementioned criteria, five fluids widely adopted by the refrigeration industry are selected: R1234yf, R1234ze, R245fa, R245ca and n-pentane. Although previous studies (see for example Wei *et al*. [9]) proposed the use of refrigerants such as R134a, R123, R141b and R142b, these are excluded from the selection process due to their high global warming potential. Table 1 lists the thermo-physical properties, the environmental impact and the hazard potential of the eligible working fluids. None of the candidates affect the ozone layer since all ODP values are close to zero; R1234yf and R1234ze have the lowest global warming potential.

Among the fluids considered, n-pentane presents the highest flammability risk, while R245fa, R245ca, and n-pentane have the highest toxicity.

Table 1. Thermodynamic properties at the critical point, ozone depleting potential (ODP), global warming potential (GWP) and hazard properties based on the ASHRAE Standard 34 of the working fluids investigated

Fluid	M_c [g mol^{-1}]	T_c [°C]	p_c [bar]	ODP	GWP	ASHRAE 34
R1234yf	114.04	94.7	33.82	0	4	A2
R1234ze	114.04	109.4	36.36	0	6	A2
R245fa	134.05	154	36.51	0	950	B1
R245ca	134.05	174.4	39.25	0	560	B1
n-pentane	72.15	196.5	33.7	0	11	B3

ASHRAE Standard 34 Refrigerant safety group classification – 1: No flame propagation, 2: Lower flammability, 3: Higher Flammability, A:Lower toxicity; B: Higher toxicity

Organic Rankine cycle modeling

The design-point problem commences with the thermodynamic cycle analysis of the system given in fig. 1(a). Such a step is accomplished by applying the first principle of Thermodynamics and the continuity equation to each plant constituent, thus yielding the calculation of the thermodynamic states at the inlet and outlet of the components. Steady-state operating conditions are assumed for the ORC turbogenerator. The mathematical model of the plant is implemented in the Matlab language, and the commercial software developed by Lemmon *et al*. [10] is utilized to calculate the thermophysical properties of the fluids.

Table 2. Parameters assumed to size the organic Rankine cycle turbogenerator and for the flat plate heat exchangers design

Variable	Value
Heat source inlet temperature	75 °C*, 120 °C**
Mass flow rate of the heat source	1.2* kg/s, 0.4** kg/s
Heat source pressure	1* bar, 3** bar
Cooling water inlet temperature	10 °C
Expander isentropic efficiency	60%
Pump hydraulic efficiency	70%
Electric generator efficiency	98%
Flat plate heat exchangers	
Plate thickness	0.4 mm
Plate thermal conductivity	15.4 W/mK
Inclination angle	30 °
Compact aspect ratio	1
Enlargement factor	1.22
Fouling resistance	0.05 m^{2}K/kW

* Case 1: flat plate solar collectors; ** Case 2: parabolic solar collectors

The cycle specifications for the two case studies, *i. e*. flat plate and parabolic solar collectors, and the design parameters of the flat plate heat exchangers are listed in tab. 2. Note that the mass flow rates of the two heat sources were chosen to limit the electric power output to 6.5 kW. Flat plate heat exchangers with herringbone corrugations are selected for the preheater, evaporator, and condenser. For small-scale and low temperature heat sources, flat plate heat exchangers are preferable compared to shell-and-tube confi-

gurations due to their compactness and high heat transfer coefficients which imply less heat transfer area [11]. Furthermore, flat plate heat exchangers are easier to maintain and have a lower tendency to fouling. The design parameters regarding the heat transfer equipment are acquired from Shah and Sekulic [12].

Flat plate heat exchanger design

The logarithmic mean temperature method is applied to calculate the heat transfer area required by the heat exchanger; see eq. (1),

$$q = F_t U A \Delta T_{lm} \tag{1}$$

where q is the heat rate, U – the overall heat transfer coefficient, A – the heat transfer area, ΔT_{lm} – the logarithm mean temperature difference, and F_t – the temperature correction factor which accounts for co-current and cross-flow. The well-established, standardized procedure outlined in [11] is adopted for the design of the heat transfer equipment, thus relating geometric quantities such as plate length and number of passes to the overall heat transfer coefficient given in eq. (1).

In the preheater and in the condenser region where sub-cooling takes place, the working fluid is in single-phase, whereas in the evaporator and in the remaining part of the condenser, a two-phase regime is attained. The correlations employed to evaluate the heat transfer coefficients in the single-phase and the two-phase region as well as the friction factor are:

– Single-phase [12]

$$\mathrm{Nu} = 0.205 \sqrt[3]{\mathrm{Pr}} \sqrt[6]{\frac{\mu}{\mu_w}} [f\,\mathrm{Re}^2 \sin(2\varphi)]^{0.374} \tag{2}$$

$$\frac{1}{\sqrt{f}} = \frac{\cos(\varphi)}{\sqrt{0.045\tan(\varphi) + 0.09\sin(\varphi) + f_0/\cos(\varphi)}} + \frac{1-\cos(\varphi)}{\sqrt{3.8 f_1}} \tag{3}$$

where Nu, Hg, and Pr are the Nusselt, Hagen, and the Prandtl numbers. The quantities μ and μ_w are the fluid viscosities calculated at the average fluid temperature and at the wall temperature, respectively. In eqs. (2) and (3) f is the friction factor, and the subscripts "0" and "1" refer to the same variable calculated at an inclination angle φ of 0° and 90°.

– Evaporation [13]

$$\mathrm{Nu} = Ge_1\,\mathrm{Re}^{Ge_2}\,\mathrm{Bo}^{0.3}\,\mathrm{Pr}^{0.4} \tag{4}$$

$$f = Ge_3\,\mathrm{Re}^{Ge_4} \tag{5}$$

where Bo and Re are the boiling and the Reynolds numbers. The quantities Ge_1, Ge_2, Ge_3, Ge_4 are four fitting constants calculated as suggested by Han *et al*. [13].

– Condensation [14]

$$\mathrm{Nu} = J_H \sqrt[3]{\mathrm{Pr}}, \tag{6}$$

$$J_H = \begin{cases} 60 & \mathrm{Re} > 1750 \\ \dfrac{75-60}{3000-1750}(\mathrm{Re}-60)+60 & \mathrm{Re} \geq 1750 \end{cases} \tag{7}$$

where J_H is the heat transfer factor. For the condensation process a constant friction factor of 2.0 is assumed for all fluids [14].

The flat plate heat exchanger design model was verified in the single- and two-phase regions using an example outlined in Coulson *et al*. [11]. The differences obtained among the models' results and the data reported in the aforementioned reference are within 1% in terms of both the overall heat transfer coefficient and pressure drops.

Multi-objective design optimization

The design of highly efficient and compact ORC turbogenerators requires an optimization routine capable of managing different conflicting targets, thus yielding the best system configuration. In the present paper, the multi-objective optimization modeled by the genetic algorithm [15] is utilized due to the benefits of optimizing simultaneously two or more functions. Furthermore, the genetic algorithm avoids the calculation of complex derivatives and enables searching for the global optima. The genetic algorithm parameters are specified as follows: population size 200, generation size 200, crossover fraction 0.8, and migration fraction 0.2. These numerical values are selected in order to ensure the repeatability of the solution when different simulations are performed.

The optimizer runs by acquiring first the array of the parameters and of the upper and lower bounds, that limit the possible values for the vectors of the optimization variables $\overline{X}$, which at hand reads:

$$\overline{X}_{\mathrm{SRC}} = [T_4,\ T_1,\ \Delta T_{\mathrm{e}},\ \Delta T_{\mathrm{c}},\ L_{\mathrm{w,p}}, N_{\mathrm{ch,p}}, b_{\mathrm{p}}, N_{\mathrm{p,p}}, L_{\mathrm{w,e}}, N_{\mathrm{ch,e}}, b_{\mathrm{e}}, N_{\mathrm{p,e}}, L_{\mathrm{w,c}}, N_{\mathrm{ch,c}}, b_{\mathrm{c}}, N_{\mathrm{p,c}}] \quad (8)$$

where the T_4 is the evaporating temperature and T_1 is the condensing temperature, while ΔT_{e} and ΔT_{c} are the evaporator and condenser minimum allowable temperature differences. To model the flat plate heat exchangers, four design variables are considered: the plate width L_{w}, the number of channels per pass N_{ch}, the mean channel spacing b and the number of passes N_{p}. The subscripts "p", "e" and "c" refer to the preheater, evaporator, and condenser, respectively.

Table 3. Lower and upper bounds for the variables involved in the multi-objective optimization. Values related to the heat exchanger geometry are set according to Kuppan [16]

Variable	Lower value	Upper value
Evaporation temperature [°C]	45	110
Condensing temperature [°C]	20	35
Evaporator minimum allowable temperature difference [°C]	5	15
Condenser minimum allowable temperature difference [°C]	5	15
Plate width [m]	0.08	0.2
Channel spacing [mm]	2	3
Number of channels per pass	1	30
Number of passes	1	4

The objective functions are the electric net power output of the ORC unit P_{el} and the sum of the heat exchanger volumes V. The array of the objective functions $\bar{J}$ can thus be formulated mathematically as:

$$\bar{J} = [-P_{el}, V] \tag{9}$$

In order to produce consistent results, reasonable upper and lower boundaries on the optimization variables are selected. The lower and upper values for each optimization variable are listed in tab. 3.

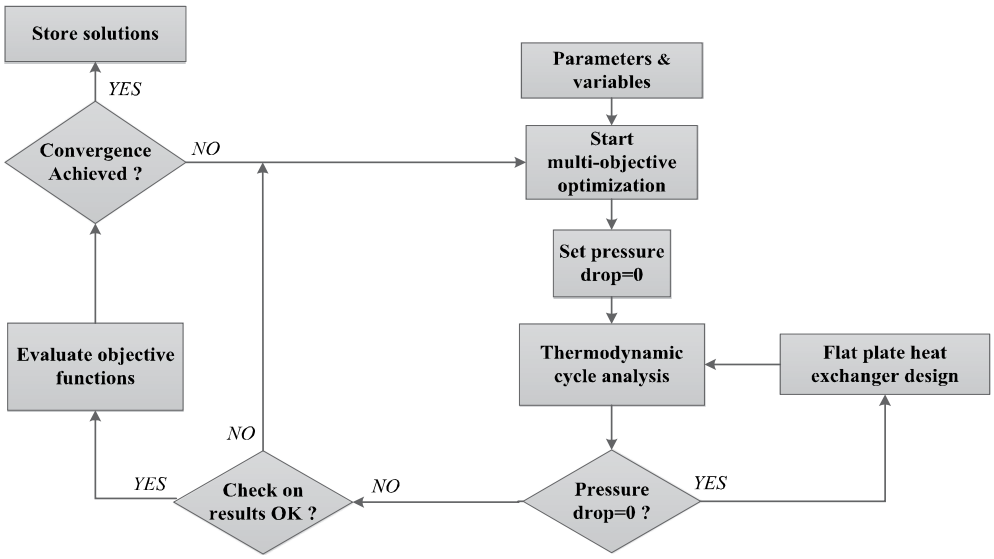

Figure 2. Structure of the multi-objective algorithm. The optimization routine involves the thermodynamic analysis of the organic Rankine cycle, the flat plate heat exchanger design, and the evaluation of the objective functions

Resuming the multi-objective design procedure (see fig. 2), the first step aims at finding the thermodynamic states at the inlet and outlet of each component using the design variables selected by the algorithm. When the operating point is calculated, it is possible to size the heat transfer equipment and to calculate the second objective function. At this stage pressure drops can be utilized to re-calculate the thermodynamic states, thus accounting for the additional pumping power required to overcome friction losses. The results are then checked with respect to the first and second principles of thermodynamics. Furthermore, it is verified that the velocity on the hot and cold sides of the heat exchangers lay within the ranges specified in Coulson *et al.* [11]. The routine terminates when the maximum number of generations is reached or when the average change of the solution is lower than the specified tolerance (10^{-3}); if this is not the case, a new calculation starts.

Results and discussion

Table 4 lists the results of the multi-objective optimization procedure applied to the second case study (parabolic plate solar collectors). The arithmetic mean average (AMA), the relative standard deviation (RSD) in percent, and the minimum and maximum values of the optimized variables are reported. A low RSD means that the variable does not change signifi-

cantly with the optimal configurations of the ORC unit. The number of passes, the mean channel spacing, the evaporating and condensing temperatures present the lowest RSD. Similar trends are obtained for the first case study (flat plate solar collectors).

Table 4. Results of the multi-objective optimization for case 2 (parabolic solar collectors). Maximum, minimum, arithmetic mean average, and relative standard deviation of the optimized variables

Variable	AMA	Minimum	Maximum	RSD [%]
T_4 [°C]	85.9	83.0	88.9	2.1
T_1 [°C]	24.6	23.5	25.4	2.1
Evaporator minimum allowable temperature difference [°C]	11.0	8.4	13.8	14.6
Condenser minimum allowable temperature difference [°C]	12.8	11.1	13.2	3.6
Preheater				
Plate width [m]	0.130	0.115	0.148	5.5
Mean channel spacing [mm]	2.23	2.21	2.32	0.9
Number of channels per pass	4.9	4	7	20.9
Number of passes	1	1	1	0.0
Evaporator				
Plate width [m]	0.13	0.10	0.18	14.5
Mean channel spacing [m]	2.29	2.20	2.74	4.1
Number of channels per pass	6.5	6	7	7.7
Number of passes	1	1	1	0.0
Condenser				
Plate width [m]	0.15	0.12	0.19	11.5
Mean channel spacing [m]	2.27	2.20	2.99	6.5
Number of channels per pass	22	17	26	10.5
Number of passes	1	1	1	0.0

Figure 3 shows the Pareto fronts obtained with the multi-objective optimization for the two case studies (see tab. 2). It can be noted that the trend of the volume *vs.* the net power output is hyperbolic. Namely, the higher the net power output, the steeper the increment in the volume of the heat transfer equipment. Hence, the solution with the highest net power output corresponds to the highest dimensions of the preheater, evaporator and condenser. Similarly, on the leftmost point, the volume and the net power generated reach their minimum values.

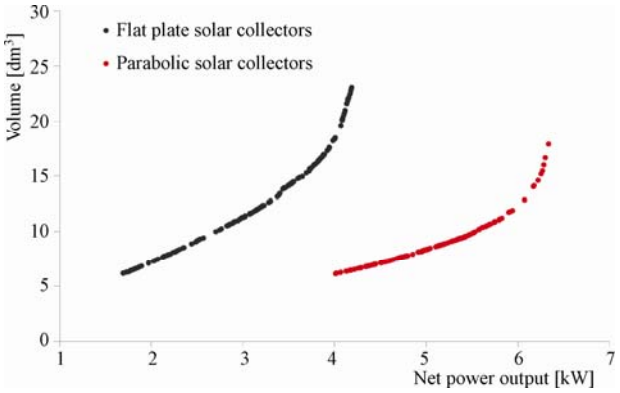

Figure 3. Pareto fronts relating the heat exchanger volume and the net power output of the ORC turbogenerator. The black-dotted line represents the case where flat plate collectors are used, while the red-dotted curve is for parabolic solar collectors

For a hot water temperature of 75 °C (flat plate solar collectors) the multi-objective optimization gives a Pareto front where the net power output ranges between 2.0 kW and 4.5 kW, while the volume varies from 6.0 dm^3 to 23.0 dm^3. In this case the

optimal working fluid is R1234yf with an optimal evaporating temperature of around 57 °C. The turbine inlet pressure is around 15.2 bar, while the condensing temperature and pressure are 22 °C and 6.3 bar, respectively. The thermal efficiency of the ORC turbogenerators exhibits a minimum value of 4.3% and a maximum value of 4.7%. A similar trend is found when parabolic solar collectors are implemented (second case study). However, in this simulation R1234ze is the optimal working fluid. The net power output generated by the system varies between 4.0 kW and 6.3 kW, whereas the volume of the heat transfer equipment ranges between 6 dm^3 and 20 dm^3. It can be noted that the optimal evaporation temperature varies between 83.0 °C and 89.0 °C, leading to an evaporation pressure between 21.4 bar and 24.2 bar. The temperature at the outlet of the condenser is around 24 °C, while the pressure is approximately 5 bar. The thermal efficiency of the ORC unit spans from 6.8% up to 7.1%. In comparison with the results of the first optimization (hot water temperature equal to 75 °C), the second Pareto front is shifted to higher net power outputs. This result is due to the higher temperature difference between the hot and the cold sources, thus consenting to boost the cycle performance. Note that the second case presents a thermal efficiency of around 7%, which is 2.5%-points higher than that obtained using flat plate solar collectors. In both cases condensation occurs at pressures (between 4 and 6 bar) above the atmospheric value; hence, the risk of air infiltrations inside the piping from the surroundings is diminished.

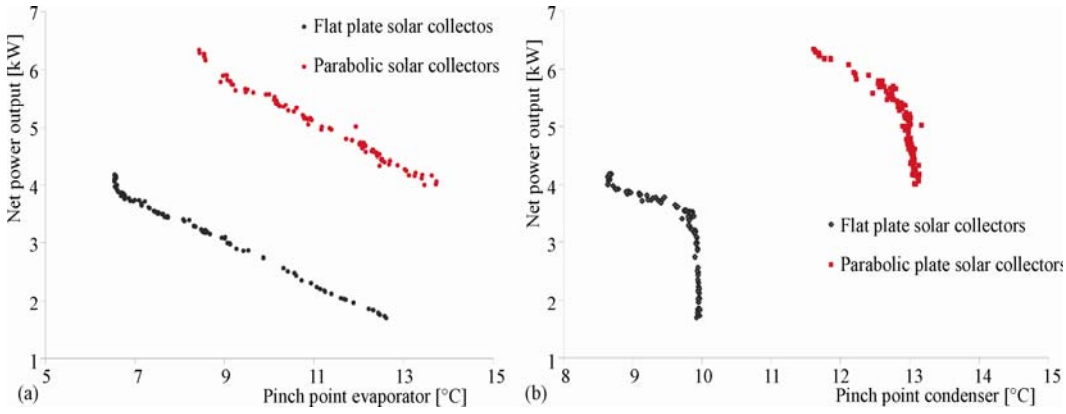

Figure 4. Minimum allowable temperature difference effect on the net power output of the ORC turbogenerator. The values are based on the Pareto front solutions. (a) Net power output *vs.* evaporator minimum allowable temperature difference; (b) Net power output *vs.* condenser minimum allowable temperature difference

Figures 4 and 5 depict the effect of the minimum allowable temperature differences (evaporator and condenser) on the net power output and heat exchanger volume for the two case studies. Such design variables have the largest impact on both objective functions. In fact, decreasing the minimum allowable temperature differences of the heat transfer equipment enhances the power production of the ORC power module by virtue of the decreased thermodynamic irreversibilities associated with the heat transfer process. On the other hand, solutions with higher minimum allowable temperature differences enhance the system compactness at the cost of a lower performance.

Regarding the relative contribution of each heat exchanger to the total volume, the calculations show that the condenser contributes with the highest share, *i. e.* 60%, compared to the preheater and the evaporator.

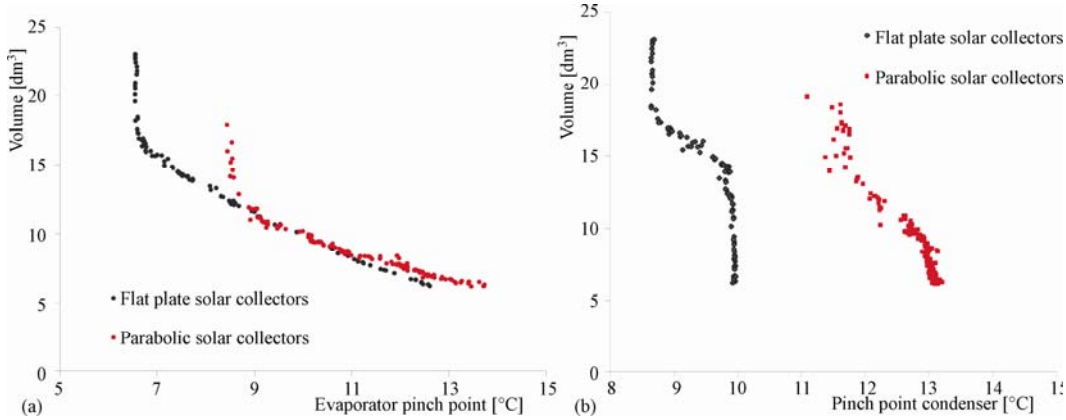

Figure 5. Minimum allowable temperature difference temperature difference effect on the heat exchanger volume. The values are based on the Pareto front solutions. (a) Heat exchanger volume versus evaporator minimum allowable temperature difference; (b) Heat exchanger volume versus condenser minimum allowable temperature difference

Such results can be explained with the relatively poor performance of the ORC turbogenerator. In fact, low thermal efficiencies imply that a large amount of heat is rejected to the environment, which in turns results in higher heat transfer areas. Moreover, values of the overall heat transfer coefficient and logarithmic mean temperature difference for the condenser are around 1,900 W/m^{2}K and 11 °C. On the contrary, higher values are encountered for the preheater (2,000 W/m^{2}K and 20 °C) and for the evaporator (2,600 W/m^{2}K and 14 °C), thus leading to lower heat transfer surfaces for a given heat rate compared to the condenser.

The results obtained in this paper are derived using various correlations, all of which are associated with uncertainties. The assumptions that have the largest influence on the results are the equations utilized to estimate the heat transfer coefficients and the pressure drops. As an example, in evaluating heat transfer coefficients, average variations of 15-20% and maximum deviations of about 40% are to be expected [17], thus influencing the volume calculation. In order to quantify the impact of variations in heat transfer coefficients and pressure drops, a sensitivity analysis is performed. Given the set of optimization variables providing the Pareto fronts shown in fig. 3, the heat transfer coefficients and the pressure drops on the organic fluid side are varied by –20% and +20%, respectively. In both case studies the largest relative deviations occur in evaluating the volume of the condenser and range from 9.2% (–2.0 dm^3) to 17.3% (3.8 dm^3). On the contrary, the variation of the evaporator volume spans from –4.1% (–0.7 dm^3) to 7.1% (0.9 dm^3). While the impact of the heat transfer coefficients on the net power output is found to be negligible, a ±20% variation of the pressure drops in condenser leads to a change in the net power output in the range of ±3.5% (±0.1 kW). Lower deviations (±0.2%) are noticed when varying the pressure drop in the evaporator. As regarding to the impact on the selection of the working fluid, preliminary investigations suggest that the optimization process discards R245fa, R245ca and n-pentane by virtue of their high critic temperatures (see tab. 1), thus leading to poor cycle performances. On the contrary,

the heat exchanger design process, which strongly relates to the adopted heat transfer and pressure drop correlations, do not influence significantly the net power output of the system and, thus, the impact of the aforementioned uncertainties on the selection of the working fluid is negligible.

Conclusions

In this study a multi-objective optimization modeled with the genetic algorithm is employed to search for optimal designs of a solar-driven organic Rankine cycle turbogenerator for domestic applications. Due to the particular case study, the major requirements of such system are high performance, compactness and safe operation. Thus, the net power output of the ORC unit and the heat exchanger volume are the specified objective functions. Considering the hot source temperature and the size of the system, the heat transfer equipment consists of three flat plate heat exchangers (preheater, evaporator and condenser) modeled with specific correlations evaluating the heat transfer coefficient and the pressure drops. The two boundary conditions considered for the hot source (liquid water) are: inlet temperature of 75 °C (flat plate solar collectors) and inlet temperature of 120 °C (parabolic solar collectors). The results indicate that the optimal working fluids are R1234yf and R1234ze for the first and for the latter case, respectively. The multi-objective optimization Pareto fronts unveil the hyperbolic relationship between the net power output of the system and the heat exchanger volume. Among the design variables considered in the optimization routine, the evaporator and condenser minimum allowable temperature differences have the largest influence on the two objective functions. The methodology presented in this paper can be employed to select the most suitable design of solar-driven ORCs by specifying the maximum volume available for the heat transfer equipment. Moreover, the outcomes of the preliminary heat exchanger design can be further utilized in the manufacturing process of organic Rankine cycle turbogenerators.

Nomenclature

A – area, [m^2]
Bo – boiling number
b – mean channel spacing [m]
c_p – heat capacity at p = const. [kJkg^{-1}K^{-1}]
d – equivalent diameter, [m]
F_t – temperature correction factor
f – friction factor
h – heat transfer coefficient, [kWm^{-2}K^{-1}]
$\overline{J}$ – array of objective functions
J_H – heat transfer factor
L – characteristic length, [m]
L_w – plate width, [m]
N_{ch} – number of channels per pass
N_p – number of passes
Nu – Nusselt number, hL/λ
P_{el} – electric net power output, [kW]
Pr – Prandtl number, $c_p\mu/\lambda$
q – heat rate, [kW]
Re – Reynolds number, $\rho ud/\mu$
T – temperature, [K]
ΔT_{lm} – logarithmic mean temperature diference, [K]
U – overall heat transfer coefficient, [kWm^{-2}K^{-1}]
V – volume, [m^3]
$\overline{X}$ – array of variables

Greek symbols

λ – thermal conductivity, [kWm^{-1}K^{-1}]
μ – viscosity, [Pa s]
ρ – density, [kgm^{-3}]
φ – inclination angle, [°]

Abbreviations

GWP – global warming potential
ODP – ozone depleting potential
ORC – organic Rankine cycle

Subscripts

0 – inclination angle equal to 0°
1 – inclination angle equal to 90°
c – condenser
e – evaporator
p – preheater
w – wall

References

[1] Quoilin, S., *et al*., Techno-Economic Survey of Organic Rankine Cycle (ORC) Systems, *Renewable and Sustainable Energy Reviews*, *22* (2013), June, pp. 168-186
[2] Tchanche, B. F., *et al*., Fluid Selection for a Low-Temperature Solar Organic Rankine Cycle, *Applied Thermal Engineering, 29* (2009), 8-9, pp. 2468-2476
[3] Quoilin, S., *et al*., Performance and Design Optimization of a Low-Cost Solar Organic Rankine Cycle for Remote Power Generation, *Solar Energy 85*, (2011), 3, pp. 955-966
[4] A. A. Lakew, O. Bolland, Working Fluids for Low-Temperature Heat Source, *Applied Thermal Engineering, 30* (2010), 10, pp. 1262-1268
[5] Larsen, U., *et al*., Design and Optimisation of Organic Rankine Cycles for Waste Heat Recovery in Marine Applications Using the Principles of Natural Selection, *Energy, 55* (2013), June, pp. 803-812
[6] Wang, J. *et al*., Multi-Objective Optimization of an Organic Rankine Cycle (ORC) for Low Grade Waste Heat Recovery Using Evolutionary Algorithm, *Energy Conversion and Management, 71* (2013), pp. 146-158
[7] Pierobon, L., *et al*., Multi-Objective Optimization of Organic Rankine Cycles for Waste Heat Recovery: Application in an Offshore Platform, *Energy, 58* (2013), Sept., pp. 538-549
[8] Trapp, C., Colonna, P., Efficiency Improvement in Precombustion CO_2 Removal Units with a Waste Heat Recovery ORC Power Plant, *Journal of Engineering for Gas Turbines and Power, 135* (2013), 4, pp. 1-12
[9] Wei, D., *et al*., Performance Analysis and Optimization of Organic Rankine Cycle (ORC) for Waste Heat Recovery, *Energy Conversion and Management 48* (2007), 4, pp. 1113-1119
[10] Lemmon, E., *et al*., Refprop: Reference Fluid Thermodynamic and Transport Properties, NIST standard reference database 23, 2007
[11] Coulson, J., *et al*., *Coulson and Richardson's Chemical Engineering, Chemical Engineering*, Butterworth-Heinemann, Oxford, UK, 1999
[12] Shah, R. K., Sekulic, D. P., *Fundamentals of Heat Exchanger Design*, John Wiley & Sons, Inc., Hoboken, USA, 2003
[13] Han, D. H., *et al*., Experiments on the Characteristics of Evaporation Of R410A in Brazed Plate Heat Exchangers with Different Geometric Configurations, *Applied Thermal Engineering*, *23* (2003), 10, pp. 1209-1225
[14] Longo, G. A., Heat Transfer and Pressure Drop During HFC Refrigerant Saturated Vapor Condensation Inside a Brazed Plate Heat Exchanger, *International Journal of Heat and Mass Transfer*, 53 (2010), 5-6, pp. 1079-1087
[15] Deb, K., *Multi-Objective Optimization Using Evolutionary Algorithms*, John Wiley & Sons, Inc., West Sussex, Great Britain, 2001.
[16] Kuppan, T., *Heat Exchanger Design Handbook*, Taylor & Francis Group, Boca Raton, Fla., USA, 2013
[17] Bonacina, C., *et al*., *Heat Transfer* (in Italian), Cleup, Padova, Italy, 1992

Paper submitted: January 22, 2014
Paper revised: April 4, 2014
Paper accepted: April 22, 2014